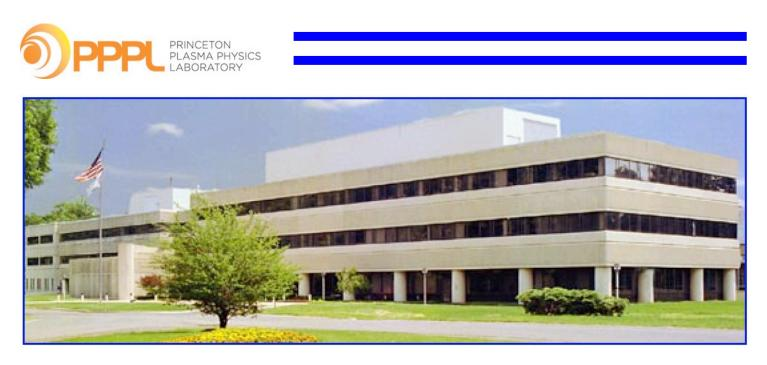
Princeton Plasma Physics Laboratory

PPPL-5271

Pressure Driven Currents Near Magnetic Islands in mD MHD Equilibria: Effects of Pressure Variation Within Flux Surfaces and of Symmetry

A. Reiman

July 2016



Prepared for the U.S.Department of Energy under Contract DE-AC02-09CH11466.

Princeton Plasma Physics Laboratory Report Disclaimers

Full Legal Disclaimer

This report was prepared as an account of work sponsored by an agency of the United States Government. Neither the United States Government nor any agency thereof, nor any of their employees, nor any of their contractors, subcontractors or their employees, makes any warranty, express or implied, or assumes any legal liability or responsibility for the accuracy, completeness, or any third party's use or the results of such use of any information, apparatus, product, or process disclosed, or represents that its use would not infringe privately owned rights. Reference herein to any specific commercial product, process, or service by trade name, trademark, manufacturer, or otherwise, does not necessarily constitute or imply its endorsement, recommendation, or favoring by the United States Government or any agency thereof or its contractors or subcontractors. The views and opinions of authors expressed herein do not necessarily state or reflect those of the United States Government or any agency thereof.

Trademark Disclaimer

Reference herein to any specific commercial product, process, or service by trade name, trademark, manufacturer, or otherwise, does not necessarily constitute or imply its endorsement, recommendation, or favoring by the United States Government or any agency thereof or its contractors or subcontractors.

PPPL Report Availability

Princeton Plasma Physics Laboratory:

http://www.pppl.gov/techreports.cfm

Office of Scientific and Technical Information (OSTI):

http://www.osti.gov/scitech/

Related Links:

U.S. Department of Energy

U.S. Department of Energy Office of Science

U.S. Department of Energy Office of Fusion Energy Sciences

Pressure Driven Currents Near Magnetic Islands in 3D MHD Equilibria: Effects of Pressure Variation Within Flux Surfaces and of Symmetry

Allan H. Reiman

Princeton Plasma Physics Laboratory, Princeton, New Jersey 08543, USA

Abstract

In toroidal, magnetically confined plasmas, the heat and particle transport is strongly anisotropic, with transport along the field lines sufficiently strong relative to cross-field transport that the equilibrium pressure can generally be regarded as constant on the flux surfaces in much of the plasma. The regions near small magnetic islands, and those near the X-lines of larger islands, are exceptions, having a significant variation of the pressure within the flux surfaces. It is shown here that the variation of the equilibrium pressure within the flux surfaces in those regions has significant consequences for the pressure driven currents. It is further shown that the consequences are strongly affected by the symmetry of the magnetic field if the field is invariant under combined reflection in the poloidal and toroidal angles. (This symmetry property is called "stellarator symmetry".) In non-stellarator-symmetric equilibria, the pressure-driven currents have logarithmic singularities at the X-lines. In stellarator-symmetric MHD equilibria, the singular components of the pressure-driven currents vanish. These equilibria are to be contrasted with equilibria having $\mathbf{B} \cdot \nabla p = 0$, where the singular components of the pressure-driven currents vanish regardless of the symmetry. They are also to be contrasted with 3D MHD equilibrium solutions that are constrained to have simply nested flux surfaces, where the pressure-driven current goes like 1/x near rational surfaces, where x is the distance from the rational surface. (Except in the case of quasi-symmetric flux surfaces.) For the purpose of calculating the pressure-driven currents near magnetic islands, we work with a closed subset of the MHD equilibrium equations that involves only perpendicular force balance, and is decoupled from parallel force balance. It is not correct to use the parallel component of the conventional MHD force balance equation, $\mathbf{B} \cdot \nabla p = 0$, near magnetic islands. Small but nonzero values of $\mathbf{B} \cdot \nabla p$ are important in this region, and small non-MHD contributions to the parallel force balance equation cannot be neglected there. Two approaches are pursued to solve our equations for the pressure driven currents. First, the equilibrium equations are applied to an analytically tractable magnetic field with an island, obtaining explicit expressions for the rotational transform and magnetic coordinates, and for the pressure-driven current and its limiting behavior near the X-line. The second approach utilizes an expansion about the X-line to provide a more general calculation of the pressure-driven current near an X-line and of the rotational transform near a separatrix. The study presented in this paper is motivated, in part, by tokamak experiments with nonaxisymmetric magnetic perturbations, where significant differences are observed between the behavior of stellarator-symmetric and non-stellarator-symmetric configurations with regard to stabilization of edge localized modes (ELMs) by resonant magnetic perturbations (RMPs). Implications for the coupling between neoclassical tearing modes (NTMs), and for magnetic island stability calculations, are also discussed.

I. Introduction

The presence of magnetic islands can have a strong influence on the performance of toroidal, magnetically confined plasmas. Pressure-driven currents near islands, in turn, play a role in determining the stability and saturated width of magnetic islands.[1,2,3] In this paper, we show that the equilibrium pressure driven current near a magnetic island can be significantly affected by the pressure variation within the flux surfaces in that region. We also show that the resulting modification of the pressure driven current is strongly affected by the symmetry of the magnetic field if the field is invariant under combined reflection in the poloidal and toroidal angles. (This symmetry property is called "stellarator symmetry".)

In toroidal, magnetically confined plasmas, the heat and particle transport is strongly anisotropic, with transport along the field lines sufficiently strong relative to cross-field transport that the equilibrium pressure can generally be regarded as constant on the flux surfaces in much of the plasma. The regions near small magnetic islands, and those near the X-lines of larger islands, are exceptions. In those regions the connection length along the field lines becomes sufficiently long that the cross-field transport can compete with the parallel transport, and there is a significant variation of the pressure within the flux surfaces.[4-8] We show in this paper that, as a consequence of the variation of the equilibrium pressure within the flux surfaces, the MHD equilibrium current driven by quasi-neutrality (the "Pfirsch-Schlüter" current) has logarithmic singularities at the X-lines in non-stellarator-symmetric equilibria. In stellarator-symmetric MHD equilibria, the singular component of the Pfirsch-Schlüter (PS) current vanishes. In contrast, in MHD equilibria having $\mathbf{B} \cdot \nabla p = 0$, the singular component of the PS current vanishes regardless of the symmetry. In 3D MHD equilibrium solutions constrained to have simply nested flux surfaces, the PS current density goes like 1/x near a rational surface, where x is the distance from the rational surface, [9-11] except in the case of quasi-symmetric flux surfaces. (See Appendix C.)

Of course, the current density is not truly singular, with additional physics that cuts off the singular behavior coming into play sufficiently close to the rational surface, or to the X-line. Some physical effects that can play this role are: field line stochasticity[12,13]; enhanced Pfirsch-Schlüter transport near the rational surface[14]; or FLR (finite Larmor radius) effects[15]. This paper deals with the situation where these effects are significant in a region which is small relative to the size of the region where there is a significant variation of the pressure within the flux surfaces. The size of the latter region is discussed below in Section II.

One conclusion of this paper is that the breakup of a rational surface to form a magnetic island can, by itself, ameliorate, but not eliminate, the singular behavior. There is a significant difference, however, in the physical implications of the two types of singularities. Unlike the 1 / x singularity, the logarithmic singularity is integrable. Even disregarding the cutoff of the

singularity, the total current contained between an island separatrix and a nearby flux surface is finite. In contrast, in the absence of a cutoff, the amount of current between an intact rational surface and any nearby flux surface is infinite. An implication is that if the cutoff of the singularity occurs sufficiently close to the singular point or singular surface, the effects of the X-line singularity are much less sensitive to the details of the cutoff than are the effects of the 1 / x singularity.

We note that there is a calculation of the pressure driven current in the neighborhood of a small magnetic island in Ref [16], taking into account the effect of the pressure variation within the flux surfaces, and the solution obtained is not singular. (It should be noted that Ref. 16 also contains several other calculations that are unaffected by this error.) The calculation of the pressure driven current in Ref. [16] is discussed in Appendix A.

For the purpose of calculating the pressure-driven currents near magnetic islands, we will work with a closed subset of the MHD equilibrium equations that involves only perpendicular force balance, and is decoupled from parallel force balance. It is not correct to use the parallel component of the conventional MHD force balance equation, $\mathbf{B} \cdot \nabla p = 0$, near magnetic islands. Small but nonzero values of $\mathbf{B} \cdot \nabla p$ are important in this region, and small non-MHD contributions to the parallel force balance equation cannot be neglected there.

The calculations described here are motivated, in part, by tokamak experiments with nonaxisymmetric magnetic perturbations, where significant differences are observed between the behavior of stellarator-symmetric and nonsymmetric configurations with regard to stabilization of edge localized modes (ELMs) by resonant magnetic perturbations (RMPs). There is evidence that the suppression of ELMs by RMPs in the DIII-D tokamak involves the penetration of the RMP at the top of the H-mode pedestal to produce a magnetic island there.[17,18] The suppression has been found to be much more difficult to achieve in a double-null configuration than in a single-null configuration. [19, 20] It has not yet been achieved for a double-null configuration in DIII-D as of the time of writing of this paper, while ELM suppression in single-null DIII-D plasmas was achieved over a decade ago.[21] As we will discuss below, tokamak configurations with a balanced double-null divertor are stellarator symmetric, while those with a single-null divertor are not.

Another instance where the question of symmetry arises is that where an island is produced by a neoclassical tearing mode (NTM) in the plasma interior. Even in a single-null tokamak, the flux surfaces may be approximately stellarator-symmetric if they are sufficiently deep in the plasma. Growth of a single island can preserve the stellarator symmetry. Growth of a second island breaks the symmetry, and the resulting modification of the pressure driven current contributes to the coupling between the NTMs. The coupling between NTMs is observed to have a significant influence on NTM growth. [22-24]

3

More generally, the Glasser-Greene-Johnson effect[25] on magnetic island stability is mediated by the Pfirsch-Schlüter (PS) current in the neighborhood of the magnetic island,[1,2,3] and it will be of interest to calculate the impact of the phenomena described in this paper on the predicted island stability.

There will be some further discussion of these phenomena in Section VIII, but it will be outside the scope of this paper to pursue a detailed investigation of these phenomena.

The subject of this paper is the effect of the pressure variation within flux surfaces on pressure driven currents near magnetic islands for stellarator-symmetric and non-symmetric MHD equilibria.

Although we focus here on the pressure driven current near a magnetic island, we note that there is a special case where the singular PS current vanishes at a rational surface even in an equilibrium having simply nested flux surfaces. This is the case where the flux surface is quasi-symmetric[26]. We will discuss this special case further in Sections IV and VII and in Appendix C.

In Section II we discuss the determinants of the pressure variation within the flux surfaces. Section III discusses the appropriate equilibrium equations for correctly handling that pressure variation. In Section IV, an analytically tractable magnetic field with an island is studied. We will see there that, for flux surfaces close to the separatrix, the region near the X-line plays a particularly important role, setting the stage for the more general calculation of Section V, which proceeds by expanding about the X-line. Section VI discusses the special case where the configuration is stellarator-symmetric about a point on the X-line. The physical interpretation of the results of the calculations are discussed in Section VII. Section VIII discusses the potential significance of the results. The main conclusions are summarized in Section IX.

II. Pressure Variation within Flux Surfaces

The pressure variation within flux surfaces is determined by a competition between parallel and perpendicular transport. When parallel transport dominates, as it usually does, the pressure may be regarded as constant on the flux surfaces. The connection length along the field lines is large near small magnetic islands, and near the X-lines of large islands, and the pressure gradient along the field lines is correspondingly small, so that the cross-field transport can dominate in those regions.

The variation of the pressure within the flux surfaces near an island is determined by the width of the island, w, relative to critical widths w_{cT} and w_{cn} for the heat and particle transport,

respectively.[4-8,27] For the case where the parallel transport is diffusive, Ref [4] defines a critical magnetic island width $w_c \equiv \sqrt{8} \left(D_{\perp} / D_{\parallel} \right)^{1/4} \left(\varepsilon_s s_s n \right)^{1/2} r_s$, where $\varepsilon_s = r_s / R_0$ is the minor radius at the rational surface divided by the major radius, $s_s = (rq' / q)_{r_s}$ is the local magnetic shear, n is the toroidal mode number of the helical perturbation, and D_{\perp} and D_{\parallel} are the corresponding cross-field and parallel diffusivities. For a low collisionality plasma, where the parallel mean-free-path is longer than the parallel wavelength of the helical perturbation, D_{\parallel} is replaced by $n_e v_e \lambda_{\parallel}$ and $n_i v_i \lambda_{\parallel}$ for heat and particle transport, respectively, where n_e and n_i are the electron and ion densities, v_e and v_i are the thermal velocities, and λ_{\parallel} is the parallel wavelength of the helical perturbation.[4-7]

For a magnetic island having width $w \ll w_{cT}$ and $w \ll w_{cn}$, the temperature and density profiles are unaffected by the presence of the island. The pressure profile is constant on the flux surfaces of the unperturbed field rather than the surfaces of the perturbed field, and there is a small but significant pressure along the perturbed field lines. For w of the order of w_{cT} or w_{cn} , the island has a significant effect on the corresponding profile. For an island with $w \gg w_{cT}$ and $w \gg w_{cn}$, the density and temperature profiles can be regarded as constant on the flux surfaces inside and outside the island, except near an X-line. In the absence of sources or sinks in the island, the profiles are flattened in the island, short–circuiting the confinement across that region of the plasma. Even for large islands, however, there are regions of radial width w_{cn} and w_{cT} about the X-line where the density and temperature, respectively, have a significant variation within the flux surfaces.[4] On flux surfaces approaching the separatrix, the field line trajectories have an increasing fraction of their length lying in close proximity to the X-line, and the connection length goes to infinity as the X-line is approached, so that perpendicular diffusion dominates in a region near the X-line.

We follow refs. [4] and [7] to obtain rough estimates for the critical scale lengths at the top of the H-mode pedestal for DIII-D shot 115467, an RMP ELM suppression shot, for which the relevant data is given in Ref. [21]. (As mentioned above, there is evidence that RMP ELM suppression involves the formation of an island at the top of the pedestal.) Although the density is relatively flat in the plasma interior, the density gradient is significant near the top of the pedestal, so that w_{cn} is the scale length that determines the region where the pressure gradient along the field lines is non-negligible. The relevant regime is that for a low collisionality plasma, and we estimate the critical scale length to be $w_{cn} \approx 1$ cm. For comparison, the ion sound radius at the top of the pedestal is approximately 0.3 cm.

III. The Equilibrium Equations

6

We turn to the question of the appropriate equations for plasma equilibria with $\mathbf{B} \cdot \nabla p \neq 0$ near magnetic islands. We will work with a closed subset of the MHD equilibrium equations that involves only perpendicular force balance, and is decoupled from parallel force balance. To motivate our approach, we consider first a steady-state force balance equation in which we retain weak anisotropic terms in the pressure tensor ($\mathbf{P} = p\mathbf{I} + \boldsymbol{\pi}$, with $|\nabla \cdot \boldsymbol{\pi}| \ll |\nabla p|$) as well as a weak flow ($|\rho_{m}\mathbf{v} \cdot \nabla \mathbf{v}| \ll |\nabla p|$, where ρ_{m} is the mass density), giving

$$\mathbf{j} \times \mathbf{B} - \nabla p = \rho_{\mathrm{m}} \mathbf{v} \cdot \nabla \mathbf{v} + \nabla \cdot \boldsymbol{\pi}. \tag{1}$$

(Details concerning the small terms that appear on the right-hand side of this equation will not matter for the purposes of this paper. A careful treatment of FLR effects can be found in Ref. 15.) The parallel component of the force balance equation is

$$\mathbf{B} \cdot \nabla p = -\mathbf{B} \cdot \big(\rho_{\mathbf{m}} \mathbf{v} \cdot \nabla \mathbf{v} + \nabla \cdot \boldsymbol{\pi} \big). \tag{2}$$

We cannot neglect the small terms on the right hand side of this equation, because they balance a small but significant pressure gradient along the field lines. The small but nonzero $\mathbf{B} \cdot \nabla p$ is important because it allows the pressure to vary within flux surfaces, and that can have a significant effect.

Writing $\mathbf{j} = j_{\parallel} \mathbf{B} / B + \mathbf{j}_{\perp}$, the cross product of \mathbf{B} with Eq. (1) gives $\mathbf{j}_{\perp} = \mathbf{B} \times \nabla p / B^2 + \mathbf{B} \times (\rho_{\mu} \mathbf{v} \cdot \nabla \mathbf{v} + \nabla \cdot \boldsymbol{\pi}) / B^2$. The small anisotropic pressure tensor term and the term arising from the weak flow make small contributions to \mathbf{j}_{\perp} , and we neglect them to get

$$\mathbf{j}_{\perp} = \mathbf{B} \times \nabla p / B^2. \tag{3}$$

The parallel component of the current is determined by $\nabla \cdot \mathbf{j} = 0$,

$$\mathbf{B} \cdot \nabla (j_{\parallel} / B) = -\nabla \cdot \mathbf{j}_{\perp}. \tag{4}$$

The equations are closed by Ampere's Law,

$$\nabla \times \mathbf{B} = \mu_0 \mathbf{j}. \tag{5}$$

Eqs. (3) - (5) is a closed set of MHD equilibrium equations that involves only perpendicular force balance, and is decoupled from parallel force balance. Eq. (2) is more properly considered to be one of the transport equations rather than one of the equilibrium equations. Note that if we take the cross product of **B** with Eq. (3) we get the equation $\mathbf{j}_{\perp} \times \mathbf{B} = \nabla p - \mathbf{B}(\mathbf{B} \cdot \nabla p) / B^2$. The parallel component of this equation vanishes identically, so Eqs. (3) – (5) are decoupled from parallel force balance, and they do define a closed set of equations. The pressure gradient can be determined by solving a set of transport equations, as before, but flux surface averaged transport equations cannot be used near magnetic islands.[8,27] Eq. (4) is a type of equation called a "magnetic differential equation", which is an equation along a magnetic field line.[28,29] The part of the current that is determined by Eq. (4) is known as the 'Pfirsch-Schlüter" (PS) current. As in any equilibrium calculation, there is a profile that must be specified that determines the constant of integration for Eq. (4).

We note that the PIES code[30,31], which calculates 3D equilibria with magnetic islands, solves equations (3) - (5), and it does not assume that the pressure is constant on the flux surfaces.

In the following, we will focus on the solution for the pressure driven current. We first solve for magnetic coordinates. In these coordinates, the magnetic differential equation determining the PS currents is a linear, first order partial differential equation with constant coefficients, which is readily solved. Two approaches will be pursued to solve for magnetic coordinates. First, in Section IV, an analytically tractable magnetic field with an island will be studied, obtaining explicit expressions for the rotational transform and magnetic coordinates, and for the pressure-driven current and its limiting behavior near the X-line. We will see that, for flux surfaces close to the separatrix, the region near the X-line plays a particularly important role, setting the stage for the calculation of Section V, which expands about the X-line to provide a more general calculation of the PS current near an X-line and of the rotational transform near a separatrix.

IV. Pressure-Driven, MHD Equilibrium Currents for an Analytically Tractable Magnetic Field with an Island.

For our analytically tractable field, we take $\mathbf{B} = \mathbf{B}_0 + \mathbf{B}_1$, where \mathbf{B}_0 is an equilibrium field with simply nested flux surfaces, and $|\mathbf{B}_1| \ll |\mathbf{B}_0|$. We adopt the usual assumptions made in analytical calculations for magnetic islands: a \mathbf{B}_1 consisting of a single resonant Fourier harmonic, and an island that is narrow relative to the macroscopic scale length, and is sufficiently narrow that the constant ψ approximation is valid. By working in flux coordinates, rather than cylindrical coordinates, we include the 3D effects that drive resonant equilibrium currents.

A. The Unperturbed Field

The 0'th order quantities satisfy equations (3) – (5), with \mathbf{B}_0 , \mathbf{j}_0 and p_0 replacing \mathbf{B} , \mathbf{j} and p in the equations. \mathbf{B}_0 can be written in terms of magnetic coordinates as[28,32,33]

$$\mathbf{B}_{0} = \nabla \psi_{t0} \times \nabla \theta_{0} + \nabla \phi \times \nabla \psi_{p0}, \qquad (6)$$

where ψ_{t0} is the unperturbed toroidal flux, and $\psi_{p0}(\psi_{t0})$ is the unperturbed poloidal flux, a function only of ψ_{t0} . The unperturbed "rotational transform", ι_0 , and the unperturbed "safety factor", q_0 , are defined by $\iota_0 \equiv d\psi_{p0} / d\psi_{t0} \equiv 1/q_0$. Eq. (6) does not uniquely specify the angular coordinates, and we complete the specification of the coordinates by taking ϕ to be the standard geometric toroidal coordinate. In this case, θ_0 is not the conventional geometric angle, but is

constructed to allow the field to be written in the canonical form of Eq. (6) while preserving the periodicity properties of the geometric poloidal angle. (These coordinates are sometimes referred to as "PEST coordinates".[34])

A coordinate system $(\psi_{10}, \theta_0, \phi)$ in which Eq. (6) holds is variously called a "magnetic coordinate system", or a "flux coordinate system with straight field lines", or a "field line following coordinate system". Magnetic coordinates have the property that the magnetic field lines are straight, in the sense that $\mathbf{B} \cdot \nabla \theta_0 / \mathbf{B} \cdot \nabla \phi$ is constant along field lines. The constant is $t_0 = 1 / q_0$. Magnetic coordinates simplify the solution of magnetic differential equations. The magnetic differential equation for the Pfirsch-Schlüter current of the unperturbed field (Eq. (4) with **B** and **j** replaced by \mathbf{B}_0 and \mathbf{j}_0) can be rewritten

$$\left(\frac{\partial}{\partial \phi} + \iota_0 \frac{\partial}{\partial \theta_0}\right) (j_{0\parallel} / B_0) = -\nabla \cdot \mathbf{j}_{0\perp} / \mathbf{B}_0 \cdot \nabla \phi.$$
(7)

Using a Fourier representation on both sides of the equation,

$$j_{0\parallel} / B_0 = \sum_{n,m} \left(j_{0\parallel} / B_0 \right)_{nm} \exp[i(m\theta_0 - n\phi)], \qquad (8)$$

etc., we get, for the Fourier terms other than the n = 0, m = 0 term,

$$\left(j_{0\parallel} / B_0\right)_{nm} = \frac{l}{l_0 m - n} \left(\nabla \cdot \mathbf{j}_{0\perp} / \mathbf{B}_0 \cdot \nabla \phi\right)_{nm}, \qquad (9)$$

where the Fourier coefficients are functions only of ψ_{10} . The n = 0, m = 0 term of Eq. (7) gives

$$\left(\nabla \cdot \mathbf{j}_{0\perp} / \mathbf{B}_0 \cdot \nabla \phi\right)_{00} = \mathbf{0},\tag{10}$$

which is a solubility condition. The solubility condition is discussed in Appendix B. As in any equilibrium calculation, there is a profile that must be specified that determines the constant of integration for Eq. (4), which corresponds to the n = 0, m = 0 term of $j_{0\parallel} / B_0$. Eq. (9) is the solution for the Pfirsch-Schlüter current.

Eq. (9) displays the well known singularity of resonant Pfirsch-Schlüter currents at rational surfaces in MHD equilibria with nested flux surfaces. The resonant Fourier components of $\nabla \cdot \mathbf{j}_{\perp} / \mathbf{B} \cdot \nabla \phi$ are in general nonzero in fully 3D equilibria. They do vanish when the field is quasi-symmetric[26] at the rational surface. (Unless *t* coincides with the helical pitch of the quasi-symmetry.) This is discussed in Appendix C.

Physically, the singularities in the Pfirsch-Schlüter current arise from the quasi-neutrality constraint. In the context of the MHD fluid equations, nonzero $\nabla \cdot \mathbf{j}_{\perp}$ produces charge accumulations which must be neutralized by currents along the field lines. Those neutralizing currents are the Pfirsch-Schlüter currents. In the context of a particle picture, the charge accumulations arise from particle drifts. At rational surfaces the field lines close on themselves,

and it is not possible to neutralize the relative charges that build up between the different closed field lines. On flux surfaces approaching the rational surface, the path followed by the neutralizing current is increasingly long, and there is a corresponding increase in the current density.

B. The Perturbed Field

We add a perturbation consisting of a single resonant Fourier component,

$$\mathbf{B}_{1} = \varepsilon \sin\left(M\theta_{0} - N\phi\right) \nabla\phi \times \nabla(M\theta_{0}), \tag{11}$$

where ε / B_0 is assumed small, and where $N / M = \iota_{0r}$ is the value of ι_0 at the rational surface expressed in lowest terms. (i.e. M and N do not have a common divisor greater than 1.) The form of the perturbation has been chosen such that $\mathbf{B}_1 \cdot \nabla \psi_{10} \neq 0$.

It will be convenient to express the magnetic field in terms of a "helical flux coordinate system". We define a helical flux function $\psi_{h0} \equiv \psi_{p0} - (N / M)\psi_{t0} + \text{constant}$, where the constant is chosen such that ψ_{h0} vanishes at the rational surface, and we define a helical angle $\theta_{h0} \equiv M\theta_0 - N\phi$. We can similarly add a constant to ψ_{t0} without affecting **B**₀. We subtract from ψ_{t0} its value at the rational surface, $\psi_{t0,r}$, and we define a normalized toroidal flux coordinate $\overline{\psi}_{t0} \equiv (\psi_{t0} - \psi_{t0,r}) / M$. Eqs. (6) and (11) then give

$$\mathbf{B} = \nabla \bar{\psi}_{t0} \times \nabla \theta_{h0} + \nabla \phi \times \nabla \psi_{h} (\bar{\psi}_{t0}, \theta_{h0}), \tag{12}$$

where

$$\psi_{h}(\bar{\psi}_{t0},\theta_{h0}) = \psi_{h0}(\bar{\psi}_{t0}) - \varepsilon \cos(\theta_{h0}), \qquad (13)$$

with $d\psi_{h0} / d\overline{\psi}_{t0} \equiv t_{h0} = Mt_0 - N$. The resonance condition becomes $t_{h0} = Mt_0 - N = 0$. It follows from Eq. (12) that $\mathbf{B} \cdot \nabla \psi_h = 0$, so the surfaces of constant ψ_h correspond to flux surfaces, and they define a magnetic island. For ε small, the island is narrow, and we assume that the region of interest is sufficiently narrow that ε may be regarded as constant in that region, the "constant psi approximation". We Taylor expand $t_{h0}(\overline{\psi}_{t0}) \approx t'_{h0} \overline{\psi}_{t0}$, giving $\psi_{h0}(\overline{\psi}_{t0}) \approx t'_{h0} \overline{\psi}_{t0}^2 / 2$, and

$$\psi_{h}(\overline{\psi}_{t0},\theta_{h0}) \approx \iota'_{h0} \,\overline{\psi}_{t0}^{2} \,/ \, 2 - \varepsilon \cos(\theta_{h0}), \tag{14}$$

where ι'_{h0} is $d\iota_{h0} / d\overline{\psi}_{t0}$ evaluated at the rational surface. (If $\varepsilon \iota'_{h0} < 0$, we shift the ϕ coordinate origin, $\phi \to \phi + \pi / N$, which reverses the sign of ε .)

The coordinate system $(\psi_h, \theta_{h0}, \phi)$ is a flux coordinate system, in the sense that $\mathbf{B} \cdot \nabla \psi_h = 0$, but it is not a magnetic coordinate system. It is easily verified from Eqs. (12) and (13) that the field lines are not straight in these coordinates.

As is usual in calculations of this sort, we will assume that the solution to Eq. (4) in the neighborhood of a narrow magnetic island is dominated by the resonant Fourier components of j_{\parallel}/B , i.e. the components (n,m) such that n = jN and m = jM for some integer j. (This is indicated by Eq. (9)). For our calculation of j_{\parallel}/B in the neighborhood of a narrow island, we will retain only the resonant components. By doing so, and by transforming to a helical magnetic coordinate system, we reduce the dimensionality of the space that we are working in. That is, we can work with a $(\overline{\psi}_{t0}, \theta_{h0})$ rather than a $(\overline{\psi}_{t0}, \theta_{h0}, \phi)$ coordinate system. The coordinate transformation, however, complicates the periodicity constraints, which must be addressed. Any physical quantity on the torus, denoted by $f(\psi_{t0}, \theta_0, \phi)$, must be a periodic function of the angles, satisfying $f(\psi_{10}, \theta_0 + 2\pi, \phi) = f(\psi_{10}, \theta_0, \phi)$ and $f(\psi_{10}, \theta_0, \phi + 2\pi) = f(\psi_{10}, \theta_0, \phi)$. In the $(\overline{\psi}_{10}, \theta_{00}, \phi)$ coordinate system these periodicity constraints assume a more complicated form: $f(\overline{\psi}_{10}, \theta_{h0} + 2M\pi, \phi) = f(\overline{\psi}_{10}, \theta_{h0}, \phi)$ and $f(\overline{\psi}_{t0}, \theta_{h0}, \phi + 2\pi) = f(\overline{\psi}_{t0}, \theta_{h0} + 2N\pi, \phi)$. With nonresonant components removed, Fourier expansions in the helical magnetic coordinate system take the form $f = \sum_{m_h} f_{m_h}^{(h)} \exp(im_h \theta_{h0})$. (We use m_h and n_h to denote mode numbers in the $(\overline{\psi}_{t0}, \theta_{h0}, \phi)$ coordinate system.) It follows that f is independent of ϕ at fixed θ_{h0} , and that $f(\overline{\psi}_{t0}, \theta_{h0} + 2\pi, \phi) = f(\overline{\psi}_{t0}, \theta_{h0}, \phi)$, so both of the required periodicity constraints are satisfied.

We caution that j_{\parallel}/B will not have a periodicity length of 2π with respect to $M\theta - N\psi$ if θ and ϕ are the geometric coordinates, nor will it be independent of ϕ at a fixed value of $M\theta - N\phi$, even close to the rational surface. We obtain these properties only by transforming to magnetic coordinates of the unperturbed field.

C. Magnetic Coordinates for the Perturbed Field

To find magnetic coordinates for the field given by Eqs. (12) and (14), we take advantage of the fact that the equations for the field line trajectories for Eq. (12) assume the form of Hamilton's equations.[35,36],

$$d\overline{\psi}_{t0} / d\phi = \mathbf{B} \cdot \nabla \overline{\psi}_{t0} / \mathbf{B} \cdot \nabla \phi = -\partial \psi_h / \partial \theta_{h0},$$
$$d\theta_{h0} / d\phi = \mathbf{B} \cdot \nabla \theta_{h0} / \mathbf{B} \cdot \nabla \phi = \partial \psi_h / \partial \overline{\psi}_{t0}.$$

These are Hamilton's equations, where ψ_h is the Hamiltonian, $\overline{\psi}_{10}$ plays the role of the momentum, θ_{h0} is the conjugate coordinate, and ϕ plays the role of time. Magnetic coordinates correspond to action-angle variables. Eq. (6) corresponds to

$$d\psi_{t0} / d\phi = \mathbf{B}_0 \cdot \nabla \psi_{t0} / \mathbf{B}_0 \cdot \nabla \phi = -\partial \psi_{\mathbf{p}0} / \partial \theta_0 = 0,$$

and

$$d\theta_0 / d\phi = \mathbf{B}_0 \cdot \nabla \theta_0 / \mathbf{B}_0 \cdot \nabla \phi = \partial \psi_{p0} / \partial \psi_{t0} = \iota_0(\psi_{t0}).$$

These are Hamilton's equations in action-angle variables. Eq. (14) corresponds to the Hamiltonian for a pendulum. This correspondence provides the magnetic coordinates we are seeking in terms of the known action-angle variables for the pendulum.[37-39]

The solution for the action-angle variables for the pendulum Hamiltonian in terms of elliptic integrals can be found in e.g. Ref [37]. We define the elliptic integral of the first kind to be $F(\chi,k) \equiv \int_0^{\chi} (1-k^2 \sin^2 \chi')^{-1/2} d\chi'$, and the elliptic integral of the second kind to be $E(\chi,k) \equiv \int_0^{\chi} (1-k^2 \sin^2 \chi')^{1/2} d\chi'$. These are the "incomplete" elliptic integrals. The corresponding complete elliptic integrals are defined as $K(k) \equiv F(\pi/2,k)$ and $E(k) \equiv E(\pi/2,k)$. We define $\rho \equiv \sqrt{(\psi_h + \varepsilon)/2\varepsilon}$. The coordinate ρ is constant on magnetic surfaces, $\rho = 0$ on the O-line of the island, $\rho < 1$ inside the island, and $\rho > 1$ outside the island.

We note that the Hamiltonian, Eq. (14), is symmetric with respect to reflection in θ_{h0} , and with respect to reflection in $\overline{\psi}_{t0}$. (We will deal with the more general case in Section V). Although the Hamiltonian is symmetric, the underlying unperturbed field, \mathbf{B}_0 , need not have these symmetry properties. It follows from the symmetry properties of the Hamiltonian that the angular magnetic coordinate of the perturbed field, θ_h , is antisymmetric with respect to the magnetic coordinates of the unperturbed field,

$$\theta_{h}\left(\overline{\psi}_{t0},-\theta_{h0}\right) = -\theta_{h}\left(\overline{\psi}_{t0},\theta_{h0}\right), \ \theta_{h}\left(-\overline{\psi}_{t0},\theta_{h0}\right) = -\theta_{h}\left(\overline{\psi}_{t0},\theta_{h0}\right).$$
(15a)

The radial magnetic coordinate, $\overline{\psi}_{i}$, is symmetric,

$$\overline{\psi}_{i}\left(-\theta_{h0},\overline{\psi}_{t0}\right) = \overline{\psi}_{i}\left(\theta_{h0},\overline{\psi}_{t0}\right), \ \overline{\psi}_{i}\left(\theta_{h0},-\overline{\psi}_{t0}\right) = \overline{\psi}_{i}\left(\theta_{h0},\overline{\psi}_{t0}\right).$$
(15b)

In the remainder of this section, and in Appendix D, we will calculate the solution for the magnetic coordinates only for $\theta_{h0} \ge 0$ and $\overline{\psi}_{t0} \ge 0$, with the understanding that the solution for the full range of θ_{h0} and $\overline{\psi}_{t0}$ is determined by the symmetry properties.

The magnetic coordinates inside the island, for $0 \le \eta_{h0} \le \pi / 2$ and $\overline{\psi}_{t0} \ge 0$, are: [37,38]

$$\overline{\psi}_{t} = \frac{8}{\pi} \sqrt{\frac{\varepsilon}{\iota_{h0}^{\prime}}} \Big[E(\rho) - (1 - \rho^{2}) K(\rho) \Big], \quad \theta_{h} = \frac{\pi}{2} F(\eta_{h0}, \rho) / K(\rho), \quad \rho < l, \quad (16)$$

where $\eta_{h0} \equiv \sin^{-1} \left[\sin(\theta_{h0} / 2) / \rho \right]$. The magnetic coordinates outside the island, for $0 \le \theta_{h0} \le \pi$ and $\overline{\psi}_{t0} \ge 0$, are:

$$\overline{\psi}_{\iota} = \frac{4}{\pi} \sqrt{\frac{\varepsilon}{\iota'_{h0}}} \rho E(1/\rho), \quad \theta_{h} = \pi F\left(\frac{\theta_{h0}}{2}, \frac{1}{\rho}\right) / K(1/\rho), \quad \rho > 1.$$
(17)

For surfaces far from the island, relative to the island width, $\rho \gg 1$, $E(1 / \rho) \rightarrow \pi / 2$ and $\overline{\psi}_{t} \rightarrow \psi_{t0}$. [40] Also $F(\theta_{h0} / 2, 1 / \rho) \rightarrow \theta_{h0} / 4$, giving $\theta_{h} \rightarrow \theta_{h0}$.

To solve the magnetic differential equation for j_{\parallel} / B using the magnetic coordinates (cf. Eq. 9) we also need to know the values of $\iota_{\rm h} = 1 / q_{\rm h} = 1 / (d\overline{\psi}_{\rm t} / d\psi_{\rm h})$ inside and outside the island. Using Eqs. (16) and (17), and the identities[40] dE(s) / ds = [E(s) - K(s)] / s and $dK(s) / ds = [E(s) - (1 - s)^2 K(s)] / [s(1 - s)^2]$, we get

$$\iota_{\rm h} = \frac{\pi \sqrt{\varepsilon \iota_{\rm h0}'}}{2K(\rho)} \tag{18}$$

inside the island, and

$$\iota_{\rm h} = \frac{\pi \rho \sqrt{\varepsilon \iota_{\rm h0}}}{K(1/\rho)},\tag{19}$$

outside the island, in the region where $\overline{\psi}_{t0} \ge 0$.

We will focus on the behavior of the pressure driven current near the separatrix. For that purpose we will use analytical expressions for the limiting value of the elliptic integrals of the first kind near the separatrix.

For the rotational transform, we use the limiting behavior of K(s) valid for $|1-s^2| \ll 1$ [41],

$$K(s) \approx \ln\left(4/\sqrt{1-s^2}\right). \tag{20}$$

For the incomplete integral of the first kind, $F(\chi, s)$, we will use two different approximations with overlapping domains of validity, whose domains of validity, taken together, cover the region of interest. For an angle χ in the range $0 \le \chi < \pi/2$,

$$F(\chi, 1) \approx \ln\left(\frac{1 + \sin(\chi)}{\cos(\chi)}\right).$$
 (21)

For s < 1, this provides a good approximation to $F(\chi, s)$ in the region where $\tan^2(\chi)(1-s^2)/s^2 \ll 1$, [42] which we will call "Region 1". For a given *s*, the approximation breaks down in a region near $\chi = \pi/2$, which includes the region near the X-line. To get a good approximation in that region, we use the identity [41]

$$F(\chi, s) + F(\xi, s) = F(\pi / 2, s) = K(s),$$
(22)

for angles χ and ξ that satisfy $\sqrt{1-s^2} \tan(\chi) \tan(\xi) = 1$. For a given χ and s such that $0 < \pi / 2 - \chi \ll 1$ and $0 < 1-s \ll 1$, we take $\xi = \tan^{-1} \left[1 / \left(\sqrt{1-s^2} \tan(\chi) \right) \right]$. This gives $(1-s^2) \tan^2(\xi) = 1 / \tan(\xi) \ll 1$, so that $F(\xi, s)$ is well approximated by Eq. (21). Eq. (22) then gives the approximation

$$F(\chi, s) \approx K(s) - \ln\left(\frac{1 + \sin(\xi)}{\cos(\xi)}\right) = K(s) - \frac{1}{2}\ln\left[\frac{1 + \sin(\xi)}{1 - \sin(\xi)}\right],$$

$$\cos(\chi) / \left[1 - s^2 \sin^2(\chi)\right]^{1/2},$$
(23)

where $\sin(\xi) = \cos(\chi) / \left[1 - s^2 \sin^2(\chi)\right]^{1/2}$.

Eqs. (16)-(21), and (23) now give us approximate expressions near the separatrix, both inside and outside the island, for the magnetic θ_h coordinate and for ι_h . In pursuing the implications, in the remainder of Section IV, we will pursue only the calculation outside the island. The calculation inside the island parallels that outside the island, and the corresponding expressions for the island interior are discussed in Appendix D.

Near the separatrix, outside the island, Eq. (20) gives

$$\iota_{\rm h} \approx \pi \sqrt{\varepsilon \iota_{\rm h0}'} / \ln \left(4 / \sqrt{\rho^2 - 1} \right). \tag{24}$$

Outside the island, in the region where $\tan^2(\theta_{h0} / 2)(\rho^2 - 1) / \rho^2 \ll 1$, ("Region1"),

$$\theta_{\rm h} \approx \pi \ln\left(\frac{1+\sin(\theta_{\rm h0}/2)}{\cos(\theta_{\rm h0}/2)}\right) / \ln\left(\frac{4}{\sqrt{\rho^2 - 1}}\right). \tag{25}$$

This is valid close to the separatrix, but not too close to the X-line. Close to the X-line, in the region where $\pi - \theta_{h0} \ll 1$ and $\rho^2 - 1 \ll 1$, ("Region 2"),

$$\theta_{\rm h} / \pi \approx 1 - \ln\left(\frac{1 + \sqrt{1 + (\rho^2 - 1)\tan^2(\theta_{\rm h0} / 2)}}{\sqrt{\rho^2 - 1}\tan(\theta_{\rm h0} / 2)}\right) / \ln\left(\frac{4}{\sqrt{\rho^2 - 1}}\right).$$
(26)

To facilitate comparison with a more general calculation to be discussed below, we make further use of our assumptions that $\pi - \theta_{h0} \ll 1$ and $(\rho^2 - 1) / \rho^2 \ll 1$, $0 < \pi - \theta_{h0} \ll 1$ to get

$$\frac{\theta_{\rm h}}{\pi} \approx 1 - \ln\left(\frac{\sqrt{4(\rho^2 - 1) + \delta\theta_{\rm h0}^2} + \delta\theta_{\rm h0}}{2\sqrt{\rho^2 - 1}}\right) / \ln\left(\frac{4}{\sqrt{\rho^2 - 1}}\right),\tag{27}$$

where $\delta \theta_{h0} \equiv \pi - \theta_{h0}$. Again, in the region of overlap between Region 1 and Region 2, Eq. (27) equals Eq. (25) in leading order. We also get

$$\iota_{\rm h} \approx \pi \sqrt{\varepsilon \iota_{\rm h0}'} / \ln\left(1 / \sqrt{\rho^2 - 1}\right). \tag{28}$$

D. The Pfirsch-Schlüter Current

Having solved for magnetic coordinates for the perturbed magnetic field, we can now use those coordinates to solve the magnetic differential equation for j_{\parallel} / B, as in Eq. (9). $\iota_{\rm h} = 0$ at the rational surface, and the resonant Fourier components in the $(\overline{\psi}_i, \theta_{\rm h}, \phi)$ coordinate system are those having toroidal mode number $n_{\rm h} = 0$ in that coordinate system.

At the end of Section IVB, we discarded nonresonant components in the $(\overline{\psi}_{t0}, \theta_{h0}, \phi)$ coordinate system, and that led us to perform the calculations of Section III.C in $(\overline{\psi}_{t0}, \theta_{h0})$ space. The magnetic coordinates for the perturbed magnetic field were obtained as a function of ψ_h and θ_{h0} in that section, and the resulting coordinates are independent of ϕ at fixed ψ_h and θ_{h0} . It follows that the lines of constant ψ_h and θ_{h0} are the same as those of constant $\overline{\psi}_i$ and θ_h . The $n_h = 0$ component of $\nabla \cdot \mathbf{j}_{\perp} / \mathbf{B} \cdot \nabla \phi$ in the $(\overline{\psi}_i, \theta_h, \phi)$ coordinate system corresponds to the average of $\nabla \cdot \mathbf{j}_{\perp} / \mathbf{B} \cdot \nabla \phi$ over ϕ at fixed $\overline{\psi}_i$ and θ_h , which is the same as the average over ϕ at fixed ψ_h and θ_{h0} . The resonant component of $\nabla \cdot \mathbf{j}_{\perp} / \mathbf{B} \cdot \nabla \phi$ in the $(\overline{\psi}_i, \theta_h, \phi)$ coordinate system is the same as that in the $(\psi_h, \theta_{h0}, \phi)$ coordinate system. The equation for j_{\parallel} / B is

$$\boldsymbol{\iota}_{\mathrm{h}} \frac{\partial}{\partial \boldsymbol{\theta}_{\mathrm{h}}} (\boldsymbol{j}_{||} / \boldsymbol{B}) = - (\nabla \cdot \mathbf{j}_{\perp} / \mathbf{B} \cdot \nabla \boldsymbol{\phi})_{\boldsymbol{\eta}_{\mathrm{h}} = 0},$$

where the $n_{\rm h} = 0$ Fourier component can be calculated in either the $(\bar{\psi}_{\iota}, \theta_{\rm h}, \phi)$ or the $(\psi_{\rm h}, \theta_{\rm h0}, \phi)$ coordinate system. In the following we will simplify our notation by defining

$$h \equiv \nabla \cdot \mathbf{j}_{\perp} / \mathbf{B} \cdot \nabla \phi, \quad \overline{h} \equiv -\left(\nabla \cdot \mathbf{j}_{\perp} / \mathbf{B} \cdot \nabla \phi\right)_{n=0}.$$
⁽²⁹⁾

Eq. (4) assumes the form

$$u_{\rm h} \frac{\partial}{\partial \theta_{\rm h}} (j_{\parallel} / B) = \overline{h}.$$
(30a)

We know the magnetic field and other physical quantities, including *h*, as a function of ψ_{t0} , θ_0 , and ϕ , but we need to integrate \overline{h} with respect to θ_h at fixed ψ_h . We express ψ_{t0} in terms of ψ_h and θ_{h0} (Eq. 14), and θ_0 in terms of θ_{h0} and ϕ , and that gives us \overline{h} as a function of ψ_h and θ_{h0} ,

$$\overline{h}\left(\psi_{\rm h},\theta_{\rm h0}\right) = \frac{1}{2M\pi} \int_0^{2M\pi} h(\psi_{\rm t0}(\psi_{\rm h},\theta_{\rm h0}),\theta_0(\theta_{\rm h0},\phi),\phi)d\phi.$$
(30b)

Eqs. (30) are valid both inside and outside the island. In the remainder of this section the calculation will specialize to the region outside the island. The corresponding calculation inside the island can be found in Appendix D.2.

In the region outside the island we can use Eqs. (30) to get

$$\iota_{\rm h} \frac{\partial}{\partial \theta_{\rm h0}} (j_{\rm H} / B) = \iota_{\rm h} \frac{\partial}{\partial \theta_{\rm h}} (j_{\rm H} / B) \frac{\partial \theta_{\rm h}}{\partial \theta_{\rm h0}} = \overline{h} (\psi_{\rm h}, \theta_{\rm h0}) \frac{\partial \theta_{\rm h}}{\partial \theta_{\rm h0}}.$$

Integrating with respect to θ_{h0} , we obtain

$$\iota_{\rm h} \frac{j_{\rm \parallel}}{B}(\psi_{\rm h}, \theta_{\rm h0}) = \int_0^{\theta_{\rm h0}} \overline{h}(\psi_{\rm h}, \theta_{\rm h0}') \frac{\partial \theta_{\rm h}(\psi_{\rm h}, \theta_{\rm h0}')}{\partial \theta_{\rm h0}'} d\theta_{\rm h0}'. \tag{31}$$

In combination with the solution for θ_h and ι_h , Eqs. (17) and (19), Eq. (31) provides a solution for the PS current outside the island in our analytically tractable magnetic field with a narrow island. In the remainder of this section we will use the expressions for the limiting values of the elliptic integrals to calculate the PS current near the island separatrix.

We divide the integral in Eq. (31) into two pieces, one whose integrand lies entirely in Region 1, and the second whose integrand lies in Region 2. For that purpose, we choose a δ such that $(\rho^2 - 1) / \rho^2 \ll \cot^2(\pi / 2 - \delta / 2) \ll 1$. Such a δ exists if $(\rho^2 - 1) / \rho^2 \ll 1$. In Region 1, the integration extends from $\theta'_{h0} = 0$ to $\theta'_{h0} = \min(\pi - \delta, \theta_{h0})$. For $\theta_{h0} \le \pi - \delta$, there is no contribution from Region 2. For $\theta_{h0} > \pi - \delta$, the integration in Region 2 extends from $\theta'_{h0} = \pi - \delta$ to $\theta'_{h0} = \theta_{h0}$.

Let
$$\theta_{h0}^{(\prime)} \equiv \min(\pi - \delta, \theta_{h0})$$
. We obtain an upper bound on the integral in Region 1:

$$\begin{vmatrix} \theta_{h0}^{(\prime)}(\psi_{h}) \\ \int_{0}^{\theta_{h0}} \overline{h}(\psi_{h}, \theta_{h0}') \frac{\partial \theta_{h}}{\partial \theta_{h0}'} d\theta_{h0}' \end{vmatrix} \leq \theta_{h}(\psi_{h}, \theta_{h0}^{(\prime)}(\psi_{h})) \max_{0 \leq \theta_{h0}' \leq \theta_{h0}^{(\prime)}(\psi_{h})} \left| \overline{h}(\psi_{h}, \theta_{h0}') \right|$$
(32)

$$\approx \pi \ln \left(\frac{1 + \sin(\theta_{h0}^{(\prime)}(\psi_{h})/2)}{\cos(\theta_{h0}^{(\prime)}(\psi_{h})/2)} \right) \max_{0 \le \theta_{h0}^{\prime} \le \theta_{h0}^{\prime\prime}(\psi_{h})} \left| \overline{h}(\psi_{h}, \theta_{h0}^{\prime}) \right| / \ln \left(\frac{4}{\sqrt{\rho^{2} - 1}} \right),$$

where we have used Eq. (25). Dividing by t_h , we conclude that the contribution of this piece of the integral to the Pfirsch-Schlüter current is bounded by

$$\frac{1}{\sqrt{\varepsilon \iota_{h0}^{\prime}}} \ln \left(\frac{1 + \sin(\theta_{h0}^{\prime\prime}(\psi_{h})/2)}{\cos(\theta_{h0}^{\prime\prime}(\psi_{h})/2)} \right) \max_{0 \le \theta_{h0}^{\prime} \le \theta_{h0}^{\prime\prime}(\psi_{h})} \left| \overline{h}(\psi_{h}, \theta_{h0}^{\prime}) \right|.$$

The Pfirsch-Schlüter current is well behaved in Region 1. It does not blow up as we approach the separatrix, despite the fact that $t_h \rightarrow 0$ as we approach the separatrix.

If $\theta_{h0} \leq \pi - \delta$, there is no contribution to the integral from Region 2. If $\theta_{h0} > \pi - \delta$, we can approximate $h(\psi_h, \theta'_{h0}) \approx h(\psi_h, \pi)$ in Region 2. Note that as ρ goes to 1, we can choose an increasingly small δ , so that the approximation becomes increasingly accurate. The contribution to the integral in Eq. (31) from Region 2 is

$$\int_{\pi-\delta}^{\theta_{h0}} \left[\overline{h}(\psi_{h},\theta_{h0}') \right] \frac{\partial \theta_{h}}{\partial \theta_{h0}'} d\theta_{h0}' \approx \left[\theta_{h}(\theta_{h0},\rho) - \theta_{h}(\pi-\delta,\rho) \right] \overline{h}(\psi_{h},\pi).$$
(33)

At $\theta_{h0} = \pi - \delta$, both Eqs. (25) and (26) are applicable, and $\theta_{h}(\pi - \delta, \rho)$ can be neglected relative to $\theta_{h}(\theta_{h0}, \rho)$ in Eq. (33). It follows that, for $\theta_{h0} > \pi - \delta$,

$$\frac{j_{\parallel}}{B} \approx \frac{1}{\sqrt{\varepsilon t_{h0}'}} \ln \left(\frac{4 \tan(\theta_{h0}/2)}{1 + \sqrt{1 + (\rho^2 - 1) \tan^2(\theta_{h0}/2)}} \right) \overline{h}(\psi_h, \pi) + \left(\frac{j_{\parallel}}{B}\right)^{(0)}$$
(34)

$$\rightarrow -\frac{1}{\sqrt{\varepsilon \iota_{h0}^{\prime}}} \ln\left(\sqrt{4(\rho^2 - 1) + \delta \theta_{h0}^2} + \delta \theta_{h0}\right) \overline{h}(\psi_h, \pi).$$
(35)

There is, in general, a logarithmic singularity as the X-line is approached, $\delta\theta_{h0} \rightarrow 0$ and $\rho \rightarrow 1$.

If the pressure were constant on the flux surfaces, $p = p(\psi_h)$, it would follow that $\nabla p = p'(\psi_h) \nabla \psi_h \rightarrow 0$ at the X-line if ∇p is finite away from the X-line. The diamagnetic current, \mathbf{j}_{\perp} in Eq. (3), would go to zero at the X-line. It would further follow from $\nabla \cdot \mathbf{j}_{\perp} = \mathbf{B} \times \nabla p \cdot \nabla (1/B^2)$ and $h \equiv \nabla \cdot \mathbf{j}_{\perp} / \mathbf{B} \cdot \nabla \phi$ that

 $\overline{h}(\psi_{\rm h},\pi) = \frac{1}{2M\pi} \int_0^{2M\pi} h(\psi_{\rm t0}(\psi_{\rm h},\pi),\theta_0(\pi,\phi),\phi)d\phi \text{ would go to zero at the X-line, and that the constant of the DS$

singular component of the PS current would vanish. It is not correct to assume that $p = p(\psi_h)$ in the neighborhood of a magnetic island.

In a more correct treatment that does not assume $p = p(\psi_h)$, the singular component of the PS current does not vanish, in general. We will see in Section VI that the singular component does vanish if the magnetic field satisfies a symmetry property known as "stellarator symmetry". Both tokamaks and stellarators often do satisfy this symmetry property, to a good approximation.

V. Expansion about the X-line.

16

Working with an analytically tractable magnetic field, we have solved for the limiting behavior of ι_h , θ_h , and j_{\parallel}/B near an island separatrix. Of particular interest are the expressions for ι_h near the separatrix, θ_h near the X-line, and j_{\parallel}/B near the X-line. In this section we will do an expansion about the X-line to calculate these quantities for a much broader set of configurations. Our calculation of ι_h and θ_h will follow that of Ref. 38, which provides additional details, beyond those provided here, on the calculation of these quantities.

For our calculation, we assume that the magnetic field has nested flux surfaces near the X-line, i.e. that the stochastic region near the X-line is sufficiently small that we can neglect it for the purposes of this calculation. We assume that we are given the magnetic field **B** in some neighborhood of the X-line, and that we are also given the shape of the flux surfaces near the X-line, specified as the level surfaces of a function. To make contact with the narrow island calculation of Section IV, we will denote that function as $\tilde{\psi}_{h0}$ (i.e. the flux surfaces correspond to surfaces of constant $\tilde{\psi}_{h0}$). We are free to add a constant to $\tilde{\psi}_{h0}$, and we take $\tilde{\psi}_{h0} = 0$ on the X-line.

Knowledge of **B** and $\tilde{\psi}_{h0}$ near the X-line will be adequate for calculating the quantities of interest. Although the rotational transform is an average of the field line pitch over a flux surface, and the pressure-driven component of j_{\parallel} / B is determined by the solution of a magnetic differential equation along a field line as it winds around the torus, near the island separatrix these quantities depend almost entirely on the properties of the flux surfaces and magnetic field near the X-line. As we have seen in Section IV, for flux surfaces sufficiently close to the separatrix, almost the entire span of the magnetic coordinate θ_h lies in the region near the X-line. This reflects the fact that field line trajectories on flux surfaces near the separatrix have an increasingly large fraction of their length in close proximity to the X-line as the flux surfaces approach the separatrix.

The calculation of Ref [38] was done in Cartesian coordinates. To make contact with our calculations for the narrow island, we work in a toroidal coordinate system, denoting the coordinates by $\tilde{\psi}_{t0}$, $\tilde{\theta}_{h0}$, and $\tilde{\phi}$, where $\tilde{\psi}_{t0}$ is a radial coordinate having $\tilde{\psi}_{t0} = 0$ on the X-line, and $\tilde{\theta}_{h0}$ is a helical angle that changes by $2M\pi$ in one poloidal transit of a flux surface, and by $2N\pi$ in one toroidal transit. We take $\nabla \tilde{\phi} = \nabla \phi$, where ϕ is the geometric toroidal angle.

We assume that a Taylor expansion of $\tilde{\psi}_{h0}$ to second order about the X-line gives an accurate representation of $\tilde{\psi}_{h0}$ in the region of interest. (Alternatively, any accurate second order polynomial representation will do.) Flux surfaces intersect at the X-line, implying that in each constant- ϕ plane, the X-point corresponds to a saddle point of $\tilde{\psi}_{h0}$, so that the linear terms vanish, $\tilde{\psi}_{h0} \approx \tilde{\psi}_{t0}^2 / a_0^2 - \tilde{\theta}_{h0}^2 / c_0^2$, where the values of a_0 and c_0 specify the shape of the flux surfaces near the X-line. In general there is also a cross-term in the second order representation, but that term can be transformed away by a rotation of coordinates,[38] and we assume that we have already made that coordinate transformation, hence the subscript "h" in $\tilde{\theta}_{h0}$.

We want to find coordinates $(\tilde{\psi}_{t}, \tilde{\theta}_{h}, \phi)$ such that the magnetic field can be written in the form

$$\mathbf{B} = \nabla \tilde{\psi}_{\mathrm{t}} \times \nabla \tilde{\theta}_{\mathrm{h}} + \nabla \phi \times \nabla \tilde{\psi}_{\mathrm{h}}, \qquad (36)$$

with $\tilde{\psi}_t$ a function only of $\tilde{\psi}_h$, $\tilde{\psi}_t = \tilde{\psi}_t(\tilde{\psi}_h)$. $\tilde{\psi}_h$ and $\tilde{\psi}_{h0}$ must define the same set of flux surfaces, so their leading order approximations can only differ by a multiplicative constant,

$$\tilde{\psi}_{\rm h} \approx \tilde{\psi}_{\rm t0}^2 / a^2 - \tilde{\theta}_{\rm h0}^2 / c^2. \tag{37}$$

Given the shape of the flux surfaces near the X-line and the magnetic field in that region, $\tilde{\psi}_{h}$ can be calculated as the flux through a ribbon winding around the X-line. More specifically, consider a ribbon one of whose edges is the X-line, with the second edge lying on a given flux surface at a fixed value of $\tilde{\theta}_{h0}$. The value of $\tilde{\psi}_{h}$ on that flux surface is calculated as the flux through the corresponding ribbon.

We transform to a hyperbolic coordinate system,

$$\tilde{\psi}_{t0} = a\tilde{\rho}\cosh(\alpha), \ \tilde{\theta}_{h0} = c\tilde{\rho}\sinh(\alpha).$$
 (38)

This gives $\tilde{\psi}_{h} = \tilde{\rho}^{2}$.

It follows from eq. (36) that $\mathbf{B} \cdot \nabla \phi = 2 \tilde{\rho} q_h \mathfrak{T}_{\rho}^{-1} \partial \tilde{\theta}_h / \partial \alpha$, where $\mathfrak{T}_{\rho} = (\nabla \tilde{\rho} \times \nabla \alpha \cdot \nabla \phi)^{-1}$, is the Jacobian for the $(\tilde{\rho}, \alpha, \tilde{\phi})$ coordinate system. Eq. (38) gives $\mathfrak{T}_{\rho} = ac \tilde{\rho} \mathfrak{T}_0$, where $\mathfrak{T}_0 = (\nabla \tilde{\psi}_{10} \times \nabla \tilde{\theta}_{h0} \cdot \nabla \phi)^{-1}$ is the Jacobian of the $(\tilde{\psi}_{10}, \tilde{\theta}_{h0}, \tilde{\phi})$ coordinate system. We are working in a narrow region about the X-line, and we can regard $B^{\phi} = \mathbf{B} \cdot \nabla \phi$ and \mathfrak{T}_0 as functions only of $\tilde{\phi}$ in that region, giving $\tilde{\theta}_h \approx (1/2)ac\mathfrak{T}_0 B^{\phi} t_h \alpha$, where we have dropped a constant of integration which is shown in Ref [38] to be of higher order. Using Eq. (38) to solve for α in terms of $\tilde{\theta}_{h0}$ and $\tilde{\psi}_h$, we get

 $q_{\rm h}\tilde{\theta}_{\rm h} \approx \frac{1}{2} \mathfrak{I}_0 B^{\phi} a c \ln \left(\frac{\sqrt{c^2 \tilde{\psi}_{\rm h} + \tilde{\theta}_{\rm h0}^2} + \tilde{\theta}_{\rm h0}}{c \sqrt{\tilde{\psi}_{\rm h}}} \right).$ (39)

In a single poloidal transit of a flux surface, $\tilde{\theta}_{h}$ increases (or decreases) by $2\pi M$. In transiting the torus one time on the $\iota \approx N / M$ surface at a fixed value of ϕ , the neighborhoods of M Xpoints are encountered, with $\tilde{\theta}_{h}$ changing by 2π for each such crossing. In traversing the interval from $\tilde{\theta}_{h0} = -\tilde{\theta}_{h0}'$ to $\tilde{\theta}_{h0} = \tilde{\theta}_{h0}'$, we get

$$2\pi q_{\rm h} \approx \Im_0 B^{\phi} a c \ln\left(\frac{2}{c\sqrt{\tilde{\psi}_{\rm h}}}\right),\tag{40}$$

where we have taken $\pi \gg \tilde{\theta}'_{\rm h0} \gg c \sqrt{\tilde{\psi}_{\rm h}}$.

For the analytically tractable case that we solved in Section IV, we had $\mathfrak{T}_0 B^{\phi} = 1$, $\theta_h = \pi - \tilde{\theta}_h$, $\theta_{h0} = \pi - \tilde{\theta}_{h0}$, $a = \sqrt{2/t'_{h0}}$, and $c = \sqrt{2/\varepsilon}$. For those values of *a* and *c*, we get $\tilde{\psi}_h = \psi_h - \varepsilon = 2\varepsilon(\rho^2 - 1)$. Substituting these values into eqs. (39) and (40), we recover eqs. (27) and (28).

Having calculated θ_h near the X-line, we can again use Eqs. (29) - (31) and (33) to calculate the Pfirsch-Schlüter current in that region. We get

$$\frac{j_{\parallel}}{B} \approx q_{\rm h} \Big[\pi - \tilde{\theta}_{\rm h}(\theta_{\rm h0}, \rho) \Big] \overline{h}(\psi_{\rm h}, \pi) \approx -\frac{1}{2} \mathfrak{I}_0 B^{\phi} ac \ln \Big(\sqrt{c^2 \tilde{\psi}_{\rm h}} + \tilde{\theta}_{\rm h0}^2 + \tilde{\theta}_{\rm h0} \Big) \overline{h}(\psi_{\rm h}, \pi) + \left(\frac{j_{\parallel}}{B} \right)^{(0)}$$
(41)

If we again substitute in the appropriate values for our narrow island case, we recover Eq. (35). Again, there is a logarithmic singularity at the X-line.

Again, as in Section IV.D, the singular component of the PS current vanishes if we assume that the pressure is constant on the flux surfaces, $p = p(\psi_h)$. However, it is not correct to assume that $p = p(\psi_h)$ near a magnetic island, and the Pfirsch-Schlüter current, in general, has a logarithmic singularity at the X-line.

There is a special set of configurations, where $\overline{h}(\psi_h, \pi)$ vanishes at the X-line, and where the singular component of Pfirsch-Schlüter current does vanish. This is the case for configurations which satisfy a symmetry property known as "stellarator symmetry" about a point on the X-line. That is the subject of Section VI.

19

VI. The Effect of Stellarator Symmetry

We will see in this section that the singular component of the PS current vanishes in MHD equilibria which satisfy a symmetry property known as "stellarator symmetry" about a point on the X-line.

Stellarator symmetry corresponds to symmetry with respect to combined reflection in θ and ϕ , where θ and ϕ are the underlying geometric poloidal and toroidal angular coordinates. We can construct the magnetic ($\overline{\psi}_{1}, \theta_{h}, \phi$) coordinates for a stellarator-symmetric configuration in a way that preserves the stellarator symmetry with respect to the coordinates, so that the symmetry properties with respect to reflection in θ_{h} and ϕ are then the same as those with respect to θ and ϕ .

For an axisymmetric configuration, stellarator symmetry implies up-down symmetry. Thus, a tokamak with a single-null divertor is not stellarator-symmetric. A tokamak with a balanced double-null divertor is stellarator symmetric, and remains so with the imposition of a nonaxisymmetric perturbing field having a single helicity. For a small perturbation that resonates at a rational surface, the nonresonant components may be small enough that they do not significantly break the symmetry.

All of the large contemporary stellarators have been designed to be stellarator-symmetric. Stellarator equilibria have intrinsic magnetic islands that preserve stellarator symmetry.[43,2] In practice, stellarators also have islands produced by "field errors" that do not preserve stellarator symmetry.

Individual quantities in stellarator-symmetric configurations may be antisymmetric or symmetric under combined reflection in θ and ϕ . The symmetry properties can be characterized in terms of the corresponding Fourier representations. A symmetric quantity can be expressed as a sum of cosines, while an antisymmetric quantity can be written as a sum of sines. If a function $f(\overline{\psi}_{1}, \theta_{h}, \phi)$ is symmetric, then it can be Fourier decomposed as $f(\overline{\psi}_{1}, \theta_{h}, \phi) = \sum_{n,m} f_{nm}(\overline{\psi}_{1}) \cos(n\phi - m\theta_{h})$. If a function $g(\overline{\psi}_{1}, \theta_{h}, \phi)$ is antisymmetric, it can be written as $g(\overline{\psi}_{1}, \theta_{h}, \phi) = \sum_{n,m} g_{nm}(\overline{\psi}_{1}) \sin(n\phi - m\theta_{h})$. Taking a θ_{h} or ϕ derivative of a quantity reverses the sign of its symmetry. Taking a derivative with respect to $\overline{\psi}_{1}$ preserves the sign.

Consideration of the symmetry properties in the $\phi = 0$ plane, particularly the symmetry properties near $\theta_{\rm h} = 0$, is a convenient way to assess the symmetry properties of individual

quantities. Thus, from the up-down symmetry of the flux surfaces in the $\phi = 0$ plane we see that $\mathbf{B} \cdot \nabla \overline{\psi}_t$ is antisymmetric in a stellarator-symmetric configuration, $\mathbf{B} \cdot \nabla \theta_h$ is symmetric, and $\mathbf{B} \cdot \nabla \phi$ is symmetric.

Taking the curl of **B**, we find that the components of **j** have the same symmetry properties as those of **B**. It follows that $\nabla \cdot \mathbf{j}_{\perp}$ is antisymmetric, as is $\nabla \cdot \mathbf{j}_{\perp} / \mathbf{B} \cdot \nabla \phi$. The contributions to the integral $\int_{0}^{2M\pi} h(\psi_{10}(\rho = 1, \theta_{h0} = \pi), \theta_{0}(\pi, \phi), \phi) d\phi = \int_{-M\pi}^{M\pi} h(\psi_{10}(\rho = 1, \theta_{h0} = \pi), \theta_{0}(\pi, \phi), \phi) d\phi$ cancel, so that the integral is zero.

VII. Discussion: Physical Interpretation

In a 3D equilibrium magnetic field, the cross-field particle drift generally drives differences in charge between different points on a flux surface. An electric field is established that drives currents to neutralize the charge. Within the MHD approximation, the local charge accumulation driven by the cross-field drifts is approximated as $-\nabla \cdot \mathbf{j}_{\perp}$, with \mathbf{j}_{\perp} given by eq. (3). The Pfirsch-Schlüter (PS) currents neutralize the charge.

In a 3D toroidal MHD equilibrium solution that is constrained to have simply nested flux surfaces, the PS current can neutralize the local charge difference between any two points on a flux surface if the surface is ergodically covered by a field line trajectory. The field line trajectories on a rational surface close on themselves, and do not ergodically cover the flux surface. A net charge difference can be established between the closed field lines, and the equilibrium solution breaks down at such a flux surface. (Except if the surface is quasi-symmetric, as discussed in Appendix C.) On flux surfaces approaching a low order rational surface, the field line trajectories become increasingly aligned with those on the rational surface, and the Pfirsch-Schlüter currents required to enforce quasi-neutrality become increasingly large. This gives rise to singular Pfirsch-Schlüter currents in 3D MHD equilibrium solutions that are constrained to have simply nested flux surfaces.[9-11]

In reality, the rational surfaces are broken to form magnetic islands. If the stochastic region at an island separatrix is sufficiently small, the magnetic field line trajectories in and near the island can be regarded as lying on 2D flux surfaces which are not simply nested. The X-line trajectories close on themselves, and the X-lines can accumulate a net charge. The MHD solution breaks down on this set of lines. On flux surfaces approaching the island separatrix, field line trajectories have an increasing fraction of their length lying in close proximity to the X-line, and the Pfirsch-Schlüter currents are again singular, in general. (See Eq. (41)).

If the field line trajectories are assumed to lie on flux surfaces, whether simply nested or not, the resonant Fourier components of the PS current density go like $1/(N-\iota M)$, where $\iota = N/M$ at the rational surface or the X-line, respectively. In an equilibrium with simply nested flux surfaces, $1/(N-\iota M)$ goes like 1/x near the rational surface, where x is the distance from the rational surface. Although $N-\iota M$ goes to zero at an island separatrix, the current density is finite on the separatrix, except at the X-line, where the current density has a logarithmic singularity as it approaches the X-line. (Eq. (41).) Of course, the current density is not truly singular, with additional physics coming into play sufficiently close to the rational surface, or to the X-line. Some physical effects that can play this role are: field line stochasticity[12,13]; enhanced Pfirsch-Schlüter transport near the rational surface[14]; or FLR effects[15].

The logarithmic singularity is fundamentally different from the 1/x singularity, in that it is integrable. In a 3D MHD equilibrium solution constrained to have simply nested flux surfaces, the amount of current contained in the region between a rational surface and a nearby flux surface is infinite. In an MHD equilibrium solution with flux surfaces that are not simply nested, the amount of current contained in the region between a magnetic island separatrix and a nearby flux surface is finite. As a consequence, if the cutoff of the singularity occurs sufficiently close to the X-line, the cutoff has only a small effect on the total current in the region near the separatrix, and the equilibrium solution is insensitive to the details of the cutoff.

In the special case where an MHD equilibrium is stellarator symmetric about a point on an Xline, i.e. is symmetric with respect to simultaneous toroidal and poloidal reflection about that point, there is an accumulation of equal and opposite charge on diametrically opposed locations on the X-line, and the charge can be neutrialized by a finite PS current on the X-line. The PS current remains finite on the flux surfaces approaching the island separatrix.

To provide a more intuitively plausible picture of the effect of stellarator symmetry, it may be helpful to consider a simple model for charge separation in a tokamak due to vertical guiding center drifts. Vertical ∇B (and curvature) drifts produce a charge separation in an axisymmetric tokamak plasma. In an up-down symmetric tokamak, the resulting charge density is equal in magnitude and opposite in sign for points at corresponding positions on opposite sides of the midplane. With the imposition of a resonant perturbation of a single helicity, the configuration remains stellarator symmetric about the points where the X-line intersects the midplane. Choosing one of those points as the coordinate origin, the charge density at points on the X-line that are on opposite sides of the origin and equidistant from it are equal in magnitude and opposite in sign. The average over the charge on the X-line is zero, and local charge neutrality can be restored by a PS current along the X-line. On the other hand, in the absence of symmetry there is, in general, a net charge on the X-line, and charge neutrality cannot be restored by a PS current along the X-line. As flux surfaces approach the separatrix, field line trajectories linger increasingly near the X-line, PS currents must flow over increasing distances to neutralize the charge on the flux surfaces, and the magnitude of the PS current density increases correspondingly.

Although stellarator symmetry is not sufficient to remove the PS current singularity in equilibrium solutions that are constrained to have nested flux surfaces, we note that there is an important special case where the singularity does vanish for such equilibria. This is the case where the rational surface is quasi-symmetric, i.e. where the Jacobian is symmetric in Boozer coordinates.[26] This is shown in Appendix C. In a quasi-symmetric magnetic field, the charge accumulation produced by $\nabla \cdot \mathbf{j}_{\perp}$ is the same on each closed field line on the rational surface, so that the net charge accumulation on each closed field line is zero, and a finite PS current can neutralize the charge differences on each closed field line. The PS currents in the neighborhood of the rational surface are well behaved.

VIII. Significance of Accurate Treatment of the Pfirsch-Schlüter (PS) Currents Near Magnetic Islands

Although it is generally desirable that PS currents in the neighborhood of magnetic islands be handled correctly, there are several phenomena which particularly call for careful handling of these currents. A detailed treatment of these phenomena is outside the scope of this paper. We will limit ourselves to describing the potential significance of an accurate PS current calculation for these phenomena.

The Glasser-Greene-Johnson[25] effect on magnetic island stability is mediated through the PS currents in the neighborhood of the island.[1-3] Any phenomenon in which magnetic island stability is an issue calls for a careful treatment of the PS currents.

All of the large contemporary stellarators are designed to be stellarator-symmetric, and they have intrinsic equilibrium islands that preserve the stellarator symmetry.[43,2] In practice, there are field errors produced by finite construction tolerances that break the stellarator symmetry. The sensitivity of the PS current near magnetic islands to loss of stellarator symmetry will increase the sensitivity of intrinsic equilibrium islands to symmetry breaking nonresonant field errors. There are also resonant field errors that produce non-stellarator-symmetric magnetic islands, and the effect of the PS current near the X-lines must be taken into account in calculating their effects.

As mentioned at the beginning of this paper, dramatic differences are seen in the response of edge localized modes (ELMs) to resonant magnetic perturbations (RMPs) in double-null vs single-null configurations. There is evidence that the formation of magnetic islands plays an important role in stabilization of ELMs by RMPs [17,18]. Double-null configurations are stellarator symmetric, while single null configurations are not. The magnetic island formation

associated with ELM stabilization is believed to occur at the top of the H-mode pedestal, near the plasma boundary, where the influence of the divertor on the shape of the magnetic surface is pronounced. The RMPs imposed in the experiments are small, and their influence on the shape of the magnetic surfaces is small, except near the rational surface, where the resonant components can significantly modify the flux surfaces. To a good approximation, the introduction of the RMP preserves the stellarator symmetry of the double null configuration. This suggests that the PS currents in the neighborhood of an island produced in a single-null configuration are significantly different from those in a double-null configuration. A careful treatment of the PS currents will be desirable in modeling the effect of the RMP.

Also mentioned at the beginning of this paper is the potential importance for coupling of neoclassical tearing modes (NTMs). Even in a tokamak with a single-null divertor, flux surfaces may be approximately up-down symmetric if they are sufficiently deep in the plasma. For an up-down symmetric flux surface in an axisymmetric tokamak, growth of a single island can preserve the stellarator symmetry. Growth of a second island breaks the symmetry, and the resulting modification of the pressure driven current contributes to the coupling between the NTMs. The coupling between NTMs is observed to have a significant influence on NTM growth. [22-24]

IX. Summary

The subject of this paper has been the calculation of pressure driven currents near magnetic islands in 3D MHD equilibria, including the effects of pressure variation within the flux surfaces, and of stellarator symmetry. Although it is generally desirable that pressure driven currents in the neighborhood of magnetic islands be handled correctly in the modeling of tokamak plasmas, there are several phenomena which particularly call for careful handling of these currents. A detailed treatment of these phenomena is outside the scope of this paper, and we have limited ourselves to describing the potential significance for these phenomena of an accurate calculation of the pressure driven currents. More specifically, the suppression of edge localized modes (ELMs) by resonant magnetic perturbations (RMPs) is widely believed to involve the generation of a magnetic island at the top of the H-mode pedestal. Dramatic differences are seen between stellarator symmetric and non-symmetric configurations in the response to RMPs. Another potential application is the coupling between two NTMs produced in a configuration where a single NTM preserves stellarator symmetry, and the second NTM breaks it. More generally, the PS currents near magnetic islands mediate the Glasser-Greene-Johnson effect on island stability.

To calculate the pressure driven currents, we have used a closed subset of the MHD equilibrium equations that involves only perpendicular force balance, and is decoupled from parallel force balance, Eqs (3) – (5). In particular, the pressure driven current is determined by Eqs. (3) and (4). It is not correct to use the parallel component of the conventional MHD force balance equation, $\mathbf{B} \cdot \nabla p = 0$, near a magnetic island. A small but nonzero value of $\mathbf{B} \cdot \nabla p$ can have a

significant effect in this region, and small non-MHD contributions to the parallel force balance equation cannot be neglected there.

The first step in the calculation of the pressure-driven currents was the calculation of magnetic coordinates. In these coordinates, the magnetic differential equation determining the Pfirsch-Schlüter (PS) currents is a linear, first order partial differential equation with constant coefficients, which is readily solved. Two approaches were pursued to solve for magnetic coordinates. First, the coordinates were calculated for an analytically tractable magnetic field with an island. For this case, we took advantage of the fact that the equations for the field line trajectories assume the form of Hamilton's equations. The Hamiltonian for the analytically tractable magnetic field corresponds to that for the pendulum. The magnetic coordinates correspond to the action-angle variables for the pendulum, and we used the known action-angle variables for the pendulum, which can be expressed in terms of elliptic integrals. Expressions for the limiting values of the elliptic integrals were used to calculate the pressure driven current near the separatrix.

The second approach utilized an expansion about the X-line to provide a more general calculation of the magnetic coordinates near an X-line and of the rotational transform near a separatrix.[38] This calculation made use of the fact that, although the Pfirsch-Schlüter current is determined by the solution of a magnetic differential equation along a field line, with the field line trajectory winding around a toroidal flux surface, the solution on flux surfaces close to the separatrix is dominated by the region near the X-line. Field line trajectories that traverse a region near an X-line linger in that region. As flux surfaces approach an island separatrix, an increasingly large fraction of each field line trajectory lies in close proximity to the X-line.

In a 3D MHD equilibrium solution that is constrained to have simply nested flux surfaces, the pressure driven current at a rational surface where t = N/M has a well known 1/(N - tM) singularity, with $N - tM \propto x$, where x is the distance to the rational surface. (The singularity may be absent in the special case where the surface is quasi-symmetric, as discussed in Appendix C.) We have found that when the surface breaks up to form an island, a 1/(N - tM) singularity generally remains at the X-line, but N - tM goes to zero logarithmically as the X-line is approached, so that the singularity is now a weaker, logarithmic singularity. The pressure driven current is finite on the separatrix, and continuous across it, except at the X-line.

In the special case where an MHD equilibrium is stellarator-symmetric about a point on the Xline, that is, symmetric with respect to simultaneous reflection in the poloidal and toroidal angles, the singular component of the PS current vanishes.

Acknowledgements. I am grateful to Per Helander for his comments on an earlier version of this manuscript. This work was supported by DOE Contract No. DEAC02-76CH03073.

(A.1)

Appendix A: Calculation of the Pressure Driven Current in the Paper of Schlutt and Hegna

We discuss here the calculation in Ref. 16 of the pressure driven current in the neighborhood of a small magnetic island. That calculation takes into account the effect of the pressure variation within the flux surfaces, and the solution obtained is not singular. (It should be noted that Ref. 16 also contains several other calculations that are unaffected by this error.)

In their Section III.B, the authors motivate the subsequent work of Sections III.D – III.F by investigating a simplified model that yields their Eq. (26) as the quasineutrality condition. They obtain a solution to this equation, their Eq. (27), for perturbing fields that satisfy the conditions

 $A_{\zeta k} / A_{\zeta 1} = J_{km,kn} / J_{m,n}$

and

$$\eta_k = \phi_k, \tag{A.2}$$

for each k. These conditions relate the amplitudes and phases, respectively, of the Fourier components of the perturbing vector potential to those of the Jacobian of the unperturbed field. This is a restrictive condition on the resonant perturbing field that is not satisfied in general. The authors concede this point.

In Section III.D the authors begin a complicated calculation to solve a more general form of the quasineutrality equation for the parallel current. After much algebra the authors arrive, in Section III.F, at their Eq. (74), which is stated to be equivalent to their Eq. (26). The authors then reproduce their Eq. (27) as Eq. (75), and they present it as the solution to Eq. (74). But we already know that this is the solution only if the magnetic field perturbation satisfies the stringent constraints of Eqs. **Error! Reference source not found.** and

Error! Reference source not found. There is no explanation. The paper proceeds as if Eq. (75) is, in fact, a general solution to Eq. (74).

Appendix B: Solubility Condition for the Magnetic Differential Equation Determining the Pfirsch-Schlüter Current

Eq. (4) is a magnetic differential equation determining the Pfirsch-Schlüter current. In magnetic coordinates, it takes the form of Eq. (9) (for $\mathbf{B} = \mathbf{B}_0$). Eq. (10) is a solubility condition for Eq. (9). The solubility condition can be formulated more generally to apply also to fields that do not have magnetic coordinates. For that purpose, we integrate the left hand side of Eq. (4) over a volume bounded by two flux surfaces and we use the identity $\mathbf{B} \cdot \nabla(j_{\parallel} / B) = \nabla \cdot [(j_{\parallel} / B)\mathbf{B}]$ to conclude that the integral is zero. That gives the solubility condition that the integral of the right-hand side of Eq. (4) over any volume bounded by two flux surfaces must vanish.

The solubility condition is automatically satisfied if $\mathbf{B} \cdot \nabla p = 0$. Integrating the right-hand-side of Eq. (4) over a volume bounded by two flux surfaces, we get an area integral over the two flux surfaces of $\hat{\mathbf{n}} \cdot \mathbf{j}_{\perp}$, where $\hat{\mathbf{n}}$ is the unit normal to the flux surface. It follows from Eq. (3) and $\hat{\mathbf{n}} = \nabla p / |\nabla p|$ that $\hat{\mathbf{n}} \cdot \mathbf{j}_{\perp} = 0$.

If $\mathbf{B} \cdot \nabla p \neq 0$, $\hat{\mathbf{n}} \cdot \mathbf{j}_{\perp} \neq 0$ on the flux surfaces in general, and the solubility condition is not automatically satisfied. From $\hat{\mathbf{n}} \cdot \mathbf{j}_{\parallel} = (j_{\parallel} / B)\hat{\mathbf{n}} \cdot \mathbf{B} = 0$, it follows that $\hat{\mathbf{n}} \cdot \mathbf{j}_{\perp} = \hat{\mathbf{n}} \cdot \mathbf{j}$, and the integral of $\nabla \cdot \mathbf{j}_{\perp}$ over a volume bounded by two flux surfaces is equal to the integral of $\nabla \cdot \mathbf{j}$ over that volume. This integral must vanish by ambipolarity. If it is nonzero, there is a buildup of charge in the region, and an electric field arises which modifies the relative transport of ions and electrons to restore ambipolarity. The solubility condition is satisfied in any physically relevant equilibrium.

Appendix C: Absence of Singular PS Current for Simply Nested Flux Surfaces that are Quasisymmetric

Section IV.A discusses the properties of an equilibrium magnetic field, denoted \mathbf{B}_0 , that has nested flux surfaces. Eq. (9) displays the well-known singularity of the resonant Pfirsch-Schlüter current at such a surface. In this appendix we show that the singular PS current is absent at a rational surface that is quasi-symmetric. It is assumed here that $\mathbf{B}_0 \cdot \nabla p_0 = 0$.

 \mathbf{B}_0 can be written in terms of Boozer coordinates as[14,44]

$$\mathbf{B}_{0} = \nabla \psi_{t0} \times \nabla \theta_{0} + \nabla \zeta_{0} \times \nabla \psi_{p0}, \qquad (C.1)$$

and

$$\mathbf{B}_{0} = I(\psi_{t0})\nabla\theta_{0} + g(\psi_{t0})\nabla\zeta_{0} + \gamma(\psi_{t0},\theta_{0},\zeta_{0})\nabla\psi_{t0}, \tag{C.2}$$

A Boozer coordinate system is a special type of magnetic coordinate system, $(\psi_{t0}, \theta_0, \zeta_0)$, such that \mathbf{B}_0 satisfies Eq. (C.2) as well as Eq. (C.1). Dotting Eq. (C.1) with $\nabla \zeta_0$ gives $\mathbf{B}_0 \cdot \nabla \zeta_0 = \nabla \psi_{t0} \times \nabla \theta_0 \cdot \nabla \zeta_0$. Dotting Eq. (C.1) with Eq. (C.2) gives $B_0^2 = \nabla \psi_{t0} \times \nabla \theta_0 \cdot \nabla \zeta_0 (g + t_0 I)$. It follows that

$$\nabla p_0 \times \mathbf{B}_0 \cdot \nabla \left(1 / B_0^2 \right) / \mathbf{B}_0 \cdot \nabla \zeta_0 = p_0'(\psi_{t0}) \left(I \frac{\partial}{\partial \zeta_0} - g \frac{\partial}{\partial \theta_0} \right) \left(1 / B_0^2 \right),$$

giving

$$\left(j_{0\parallel} / B_0\right)_{nm} = \frac{dp_0}{d\psi_{10}} \frac{mg + nI}{\iota_0 m - n} \left(1 / B_0^2\right)_{nm},\tag{C3}$$

if $n \neq 0$ or $m \neq 0$. The n = 0, m = 0 component of $j_{0\parallel} / B_0$ is determined, as discussed in Section IV.A, by the specified profile of net current.

A quasisymmetric flux surface is one where $1/B_0^2$ is axisymmetric or helically symmetric when expressed in Boozer coordinates.[26] The resonant Fourier components of $1/B_0^2$ vanish at a quasisymmetric flux surface, except possibly at surfaces where the helical pitch of the field line matches that of the symmetry direction, as is also possible in a helical configuration.

A large aspect ratio, analytic equilibrium calculation finds that quasisymmetry can only be satisfied exactly at one flux surface, unless the configuration is strictly symmetric.[45] The deviation from quasisymmetry of the other surfaces is third order in the inverse aspect ratio, so that the resonant Fourier components are generally small at those flux surfaces, relative to those of a non-quasi-symmetric configuration.

Appendix D: Calculations Inside the Island for the Analytically Tractable Field

From Eqs. (16) and (17) it can be seen that the expression for $\theta_{\rm h}$ outside the island maps to that inside the island if we make the substitutions $\theta_{\rm h0} / 2 \rightarrow \eta_{\rm h0}$, $\rho \rightarrow 1 / \rho$, $\theta_{\rm h} \rightarrow 2\theta_{\rm h}$. Similarly, the expression for $\iota_{\rm h}$ outside the island maps to that inside the island if we take $\rho \rightarrow 1 / \rho$ and $\iota_{\rm h} \rightarrow 2\rho \iota_{\rm h}$. We take advantage of this in the following.

1. Limiting Values of the Magnetic Coordinates Near the Separatrix

Near the separatrix, inside the island, Eq. (24) gives

$$\iota_{\rm h} \approx \frac{\pi}{2} \sqrt{\varepsilon \iota_{\rm h0}'} / \ln \left(\frac{4}{\sqrt{1 - \rho^2}} \right).$$
 (D1)

Inside the island, in the region where $(1 - \rho^2) \tan^2(\eta_{h0}) \ll 1$, ("Region1"),

$$\theta_{\rm h} \approx \frac{\pi}{2} \ln\left(\frac{1+\sin(\eta_{\rm h0})}{\cos(\eta_{\rm h0})}\right) / \ln\left(\frac{4}{\sqrt{1-\rho^2}}\right). \tag{D2}$$

In the region where $\pi / 2 - \eta_{h0} \ll 1$ and $1 - \rho^2 \ll 1$, ("Region 2"),

$$\frac{2}{\pi}\theta_{\rm h} \approx 1 - \ln\left(\frac{\sqrt{1 + (1 - \rho^2)\tan^2\eta_{\rm h0}} + 1}{\sqrt{1 - \rho^2}\tan\eta_{\rm h0}}\right) / \ln\left(4 / \sqrt{1 - \rho^2}\right).$$

Again we can make further use of our approximations to get

$$\frac{2}{\pi}\theta_{\rm h} \approx 1 - \ln\left(\frac{\sqrt{1-\rho^2 + \delta\eta_{\rm h0}^2} + \delta\eta_{\rm h0}}{\sqrt{1-\rho^2}}\right) / \ln\left(\frac{4}{\sqrt{1-\rho^2}}\right),\tag{D3}$$

where $\delta \eta_{h0} \equiv \pi / 2 - \eta_{h0}$.

2. The Pfirsch-Schlüter Current

Eqs. (30) are valid also inside the island. For the region inside the island, we define

$$h_{i}(\psi_{\mathrm{h}},\eta_{\mathrm{h0}}) \equiv h(\psi_{\mathrm{h}},\theta_{\mathrm{h0}}(\psi_{\mathrm{h}},\eta_{\mathrm{h0}})).$$

We then get

$$\iota_{\rm h} \frac{\partial}{\partial \eta_{\rm h0}} (j_{\parallel} / B) = \iota_{\rm h} \frac{\partial}{\partial \theta_{\rm h}} (j_{\parallel} / B) \frac{\partial \theta_{\rm h}}{\partial \eta_{\rm h0}} = \overline{h}_{t} (\psi_{\rm h}, \eta_{\rm h0}) \frac{\partial \theta_{\rm h}}{\partial \eta_{\rm h0}}.$$

Integrating with respect to η_{h0} , we obtain

$$\iota_{\rm h} \frac{j_{\parallel}}{B}(\psi_{\rm h},\eta_{\rm h0}) = \int_0^{\eta_{\rm h0}} \overline{h}_i(\psi_{\rm h},\eta_{\rm h0}') \frac{\partial \theta_{\rm h}(\psi_{\rm h},\eta_{\rm h0}')}{\partial \eta_{\rm h0}'} d\eta_{\rm h0}'. \tag{D4}$$

We now place the border between Region 1 and Region 2 at $\eta = \pi/2 - \delta$, where δ satisfies $(\rho^2 - 1)/\rho^2 \ll \cot^2(\pi/2 - \delta) \ll 1$.

As in Eq. (32), we obtain a bound on the integral in Region 1 showing that the PS current does not blow up as we approach the separatrix in this region.

Eq. (33) becomes

$$\int_{\pi/2-\delta}^{\eta_{h0}} \left[\overline{h}_{i}(\psi_{h},\eta_{h0}') \right] \frac{\partial \theta_{h}}{\partial \eta_{h0}'} d\eta_{h0}' \approx \left[\theta_{h}(\eta_{h0},\rho) - \theta_{h}(\pi/2-\delta,\rho) \right] \overline{h}_{i}(\psi_{h},\pi/2).$$

For $\eta_{h0} > \pi / 2 - \delta$, this gives

$$\frac{j_{\parallel}}{B} \approx \frac{1}{\sqrt{\varepsilon t_{h0}'}} \ln\left(\frac{4\tan(\eta_{h0})}{1 + \sqrt{1 + (1 - \rho^2)\tan^2(\eta_{h0})}}\right) \overline{h_i}(\psi_h, \pi/2) + \left(\frac{j_{\parallel}}{B}\right)^{(0)}.$$
(D5)

One can similarly carry through the expansion about the X-line for the region inside the magnetic island.

29

References

- [1] M. Kotschenreuther, R.D. Hazeltine, and P.J. Morrison, Phys. Fluids 28, 294 (1985).
- [2] J.R. Cary, and M. Kotschenreuther, Phys. Fluids 28, 1392 (1985).
- [3] C. C. Hegna and A. Bhattacharjee, Phys. Fluids B 1, 392 (1989).
- [4] R. Fitzpatrick, Phys. Plasmas 2, 825 (1995).
- [5] N. N. Gorelenkov, R. V. Budny, Z. Chang, M. V. Gorelenkova, and L. E. Zakharov, Phys. Plasmas **3**, 3379 (1996).
- [6] T. A. Gianakon, C. C. Hegna, and J. D. Callen, Phys. Plasmas 3, 4637 (1996).
- [7] R. D. Hazeltine, P. Helander and Catto, Phys. Plasmas 4, 2920 (1997).
- [8] M. Hölzl, S. Günter, Q. Yu, and K. Lackner, Phys. Plasmas 14, 052501 (2007).
- [9] S. Hamada, Nucl. Fusion 2, 23 (1962).
- [10] H. Grad, Phys. Fluids 10, 137 (1967).
- [11] LS. Solov'ev and V.D. Shafranov in Reviews of Plasma Physics, vol. 5, M.A. Leontovich,
- ed., Consultants Bureau, N.Y. 1970. (Original Russian text published in 1967.)
- [12] A. Reiman, M.C. Zarnstorff, D. Monticello, A. Weller, J. Geiger and the W7-AS Team, Nucl. Fusion **47**, 572 (2007).
- [13] J. A. Krommes and A. H. Reiman, Phys. Plasmas, 16, 072308 (2009).
- [14] A.H. Boozer, Phys. Fluids 24, 1999 (1981).
- [15] R. D. Hazeltine and P. J. Catto, Phys. Plasmas 22, 092513 (2015).
- [16] M. G. Schlutt and C. C. Hegna, Phys. Plasmas 19, 082514 (2012).

[17] M. R. Wade, R. Nazikian, J. S. deGrassie, T. E. Evans, N.M. Ferraro, R.A. Moyer, D.M. Orlov, R.J. Buttery, M.E. Fenstermacher, A.M. Garofalo1, M.A. Lanctot, G.R. McKee, T.H. Osborne, M.A. Shafer, W.M. Solomon, P.B. Snyder, W. Suttrop, A. Wingen, E.A. Unterberg and L. Zeng, Nucl. Fusion 55, 023002 (2015).

[18] R. Nazikian, C. Paz-Soldan, J. D. Callen, J. S. deGrassie, D. Eldon, T. E. Evans, N. M. Ferraro, B. A. Grierson, R. J. Groebner, S. R. Haskey, C. C. Hegna *et al*, Phys. Rev. Lett. **114**, 105002 (2015).

- [19] B. Hudson, T. Evans, C. Petty and P. Snyder, Nucl. Fusion 50, 064005 (2010).
- [20] T. Evans, personal communication (2015).
- [21] T.E. Evans, R.A. Moyer, J.G. Watkins, T.H. Osborne, P.R. Thomas, M. Becoulet, J.A.
- Boedo, E.J. Doyle, M.E. Fenstermacher, K.H. Finken et al, Nucl. Fusion 45, 595 (2005).
- [22] Q. Yu, S. Günter, K. Lackner, A. Gude, M. Maraschek, Nucl. Fusion 40, 2031 (2000).
- [23] E. D. Fredrickson, Phys. Plasmas 9, 548 (2002).
- [24] O Sauter, R J Buttery, R Felton, T C Hender, D F Howell and contributors to the EFDA-JET Workprogramme, Plasma Phys. Control. Fusion **44**, 1999 (2002).
- [25] A.H. Glasser, J.M. Greene, and J.L. Johnson, Phys. Fluids 18, 875 (1975).
- [26] J, Nührenberg and R. Zille, Physics Letters A 129, 113 (1988).
- [27] M. Hölzl, S. Günter, and Asdex Upgrade Team, Phys. Plasmas 15, 072514 (2008).
- [28] M.D. Kruskal and R.M. Kulsrud, Phys. Fluids 1, 265 (1958).
- [29] W.A. Newcomb, Phys. Fluids 2, 362 (1959).
- [30] Reiman A.H. and Greenside H., Comput. Phys. Commun. 43, 157 (1986).

[31] Monticello D., Reiman A. and Raburn D., Bull. Am. Phys. Soc. 58, 258 (2013).

[32] S. Hamada, Progr. Theoret. Phys. 22, 145 (1959).

[33] J. M. Greene and J. L. Johnson, Physics of Fluids 5, 510 (1962).

[34] R.C. Grimm, J.M. Greene, J.L. Johnson, Meth. Comput. Phys., 9 (1976), p. 253.

[35] J.R. Cary and R.G. Littlejohn, Annals of Physics 151, 1 (1983).

[36] A.H. Boozer, Phys. Fluids 26, 1288 (1983).

[37] A.J. Lieberman and M.A. Lichtenberg, *Regular and Chaotic Dynamics*, Springer-Verlag 1992.

[38] A.H. Reiman, N. Pomphrey and A.H. Boozer, Phys. Fluids B 1, 555 (1989).

[39] A. H. Reiman and N. Pomphrey, J. Comput. Phys. 94, 225 (1991).

[40] B. C. Carlson in "NIST Handbook of Mathematical Functions", edited by F. W. J. Olver, D.

W. Lozier, R. F. Boisvert and C. W. Clark, NIST and Cambridge University Press, 2010.

[41] L. Milne-Thomson in "Handbook of Mathematical Functions", edited by M. Abramowitz and I. Stegun, Dover Publications Inc., New York, 1965.

[42] H. Van de Vel, Mathematics of Computation, Vol. 23, No. 105 (Jan., 1969), pp. 61-69.

[43] A. H.. Reiman and A. H. Boozer, Phys. Fluids 27, 2446 (1984).

[44] A. H. Boozer, Phys. Fluids 23, 904 (1980).

[45] D. A. Garren and A. H. Boozer, Phys. Fluids B 3, 2822 (1991).



Princeton Plasma Physics Laboratory Office of Reports and Publications

Managed by Princeton University

under contract with the U.S. Department of Energy (DE-AC02-09CH11466)

P.O. Box 451, Princeton, NJ 08543 Phone: 609-243-2245 Fax: 609-243-2751 E-mail: publications@pppl.gov Website: http://www.pppl.gov